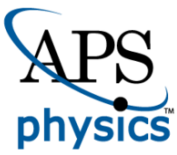



# Black-Box Superconducting Circuit Quantization

Simon E. Nigg, Hanhee Paik, Brian Vlastakis, Gerhard Kirchmair, S. Shankar, Luigi Frunzio, M. H. Devoret, R. J. Schoelkopf, and S. M. Girvin

Phys. Rev. Lett. **108**, 240502 — Published 12 June 2012

DOI: 10.1103/PhysRevLett.108.240502

# Black-box superconducting circuit quantization

Simon E. Nigg, Hanhee Paik, Brian Vlastakis, Gerhard Kirchmair, S. Shankar,
Luigi Frunzio, M. H. Devoret, R. J. Schoelkopf and S. M. Girvin
*Departments of Physics and Applied Physics, Yale University, New Haven, CT 06520, USA*

We present a semi-classical method for determining the effective low-energy quantum Hamiltonian of weakly anharmonic superconducting circuits containing mesoscopic Josephson junctions coupled to electromagnetic environments made of an arbitrary combination of distributed and lumped elements. A convenient basis, capturing the multi-mode physics, is given by the quantized eigenmodes of the linearized circuit and is fully determined by a classical linear response function. The method is used to calculate numerically the low-energy spectrum of a 3D-transmon system, and quantitative agreement with measurements is found.

PACS numbers: 42.50.Ct,85.25.Am,42.50.Pq,03.67.-a

Superconducting electronic circuits containing nonlinear elements such as Josephson junctions (JJs) are of interest for quantum information processing [1, 2], due to their nonlinearity and weak intrinsic dissipation. The discrete low-energy spectrum of such circuits can now be measured to a precision of better than one part per million [3]. The question thus naturally arises of how well one can theoretically model such man-made artificial atoms. Indeed, increasing evidence indicates that due to increased coupling strengths [4], current models are reaching their limits [5–9] and in order to further our ability to design, optimize and manipulate these systems, developing models beyond these limits becomes necessary. This is the goal of the present work.

An isolated ideal JJ has only one collective degree of freedom: the order parameter phase difference $\varphi$ across the junction. The zero-temperature, sub-gap physics of this system, with Josephson energy $E_J$ and charging energy $E_C$, is described by the Cooper-pair box Hamiltonian

$$H_{\rm CPB} = 4E_C(\hat{N} - N_g)^2 - E_J\cos(\hat{\varphi}), \qquad (1)$$

where $\hat{N}$ is the Cooper-pair number operator conjugate to $\hat{\varphi}$ and $N_g$ an offset charge. This model is exactly solvable in terms of Mathieu functions [10, 11]. The crucial feature that emerges from this solution is that the charge dispersion, i.e. the maximal variation of the eigenenergies with $N_g$, is *exponentially* suppressed with $E_J/E_C$ while the relative anharmonicity decreases only algebraically with a slow power-law in $E_J/E_C$. As a consequence, there exists a regime with $E_J \gg E_C$ – the transmon regime – where the anharmonicity is much larger than the linewidth (e.g. due to fluctuation of the offset charge $N_g$), thus satisfying the operability condition of a qubit [12]. This is the regime of interest here.

In order to be useful for quantum information processing tasks, several Josephson qubits must be made to controllably interact with each other and spurious interactions with uncontrolled (environmental) degrees of freedom must be minimized. In circuit quantum electrodynamics [2, 11, 13] (cQED), this is achieved by coupling the JJs to a common microwave environment with a desired discrete mode structure. So far such systems have mostly been described theoretically by models well known from quantum optics such as the single-mode Jaynes-Cummings model and extensions thereof [14].

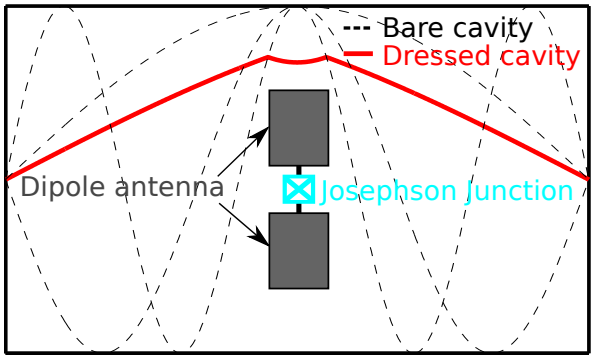


FIG. 1. (Color online) Cartoon of a JJ at the center of a broadband dipole antenna inside a 3D microwave cavity. The presence of the antenna alters the geometry of all cavity modes. This is illustrated with the lowest energy dressed mode (full (red) curve). Capturing this effect in the usual method would require the inclusion of many bare modes of the empty cavity (dashed curves). This resummation is done automatically in the method presented here.

When applied to superconducting circuits with multilevel artificial atoms, multi-mode cavities and increased coupling strengths [4, 6, 7] however, several technical and practical difficulties with these approaches arise. For example, capturing important effects of non-computational qubit states requires going to high orders in perturbation theory [15]. Also, determining the *bare* Hamiltonian parameters, in terms of which these models are defined, is cumbersome and requires iterating between experiment and theory. Perhaps even more important are the shortcomings of the traditional approaches in dealing with the multiple modes of the cavity. Indeed high-energy, off-resonant cavity modes have already been measured

to contribute substantially to the inter-qubit interaction strength [8, 15] and, via the multi-mode Purcell effect, to also affect the coherence properties (relaxation and decoherence) of the qubits [5]. Attempts at including this multi-mode physics in the standard models however, lead to difficulties with diverging series and QED renormalization issues [8], which to the best of our knowledge remain unresolved. Fig. 1 illustrates the origin of the problem with the example of a JJ inside a 3D cavity (3D-transmon) [3]. The presence of a relatively large metallic dipole antenna [16] can strongly alter the geometry of the cavity modes. This essentially classical effect, can be accounted for precisely only by including a sufficiently large number of bare modes.

In contrast, we propose to start by considering the coupled but *linearized* problem in order to find a basis that incorporates the main effects of the coupling between multi-level qubits and a multi-mode cavity and then account for the weak anharmonicity of the Josephson potential perturbatively. The crucial assumption made here is that charge dispersion effects can be safely neglected. This is reasonable given that in state-of-the art implementations of transmon qubits [3, 17], charge dispersion only contributes a negligible amount to the measured linewidths. Previous work discussed the nonlinear dynamics of a JJ embedded in an external circuit classically [18]. Here we go one step further and show how the knowledge of a classical, in principle measurable, linear response function lets us quantize the circuit, treating qubits and cavity on equal footing.

*Single junction case.* We consider a system with a JJ with *bare* Josephson energy $E_J$ and charging energy $E_C$, in parallel with a linear but otherwise arbitrary electromagnetic environment as depicted in Fig. 2 (a). Neglecting dissipation, the unbiased junction alone is described by the Hamiltonian (1). At low energies, when $E_J \gg E_C$, quantum fluctuations of the phase $\varphi$ across the junction are small compared with $\pi$ and, as emphasized in the introduction, the probability of quantum tunneling of the phase between minima of the cosine potential is negligibly small. It is then reasonable to expand the latter in powers of $\varphi$, thus obtaining the approximate circuit representation of Fig. 2 (b), in which the spider symbol [18] represents the purely nonlinear part and $L_J = {\phi_0}^2/E_J$ and $C_J = e^2/(2E_C)$ the linear parts of the Josephson element. Here $\phi_0 = \hbar/(2e)$ is the reduced flux quantum. To leading order, the energy of the spider element is given by $E_{\rm nl} = -{\phi_0}^2\varphi^4/(24L_J)$.

A quantity of central importance in the following is the impedance $Z(\omega)$ of the linear part of the circuit depicted in Fig. 2 (c). The latter is a complex meromorphic function and by virtue of Foster's theorem [19, 20] can be synthesized by the equivalent circuit of parallel LCR

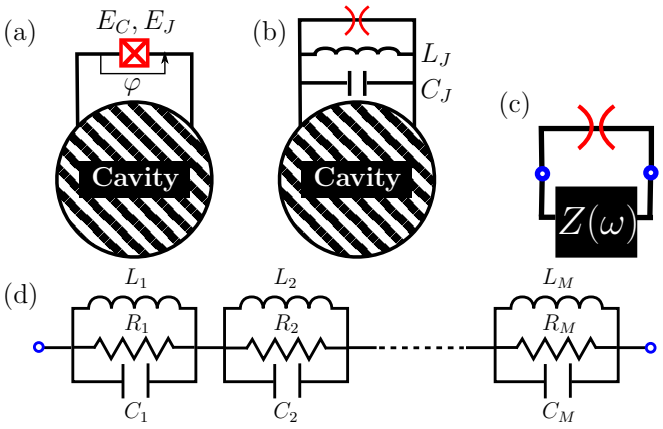


FIG. 2. (Color online) (a) Schematics of a JJ ((red) boxed cross) coupled to an arbitrary linear circuit (striped disk). (b) The Josephson element is replaced by a parallel combination of: a linear inductance $L_J$, a linear capacitance $C_J$ and a purely nonlinear element with energy $E_J(1-\cos(\varphi)) - (E_J/2)\varphi^2$, represented by the spider symbol. (c) The linear part of the circuit shown in (b) is lumped into an impedance $Z(\omega)$ seen by the nonlinear element. (d) Foster-equivalent circuit (pole-decomposition) of the impedance $Z(\omega)$.

oscillators in series shown in Fig. 2 (d). Explicitly

$$Z(\omega) = \sum_{p=1}^{M} \left( j\omega C_p + \frac{1}{j\omega L_p} + \frac{1}{R_p} \right)^{-1}, \qquad (2)$$

where $M$ is the number of modes [21] and we have adopted the electrical engineering convention of writing the imaginary unit as $j = -i$. This equivalent circuit mapping corresponds, in electrical engineering language, to diagonalizing the linearized system of coupled harmonic oscillators. The resonance frequencies of the linear circuit are determined by the real parts of the poles of $Z$ or more conveniently by the real parts of the zeros of the admittance defined as $Y(\omega) = Z(\omega)^{-1}$, and for weak dissipation, i.e. $R_p \gg \sqrt{L_p/C_p}$, are given by $\omega_p = (L_pC_p)^{-\frac{1}{2}}$. The imaginary parts of the roots $(2R_pC_p)^{-1}$, give the resonances a finite width. The effective resistances are given by $R_p = 1/\mathrm{Re}Y(\omega_p)$ and the effective capacitances are determined by the frequency derivative on resonance of the admittance as $C_p = (1/2)\mathrm{Im}Y'(\omega_p)$. Here and in the following the prime stands for the derivative with respect to frequency. Note that $\mathrm{Im}Y'(\omega) > 0$ [19]. Together this yields a compact expression for the quality factor of mode $p$:

$$Q_p = \frac{\omega_p}{2} \frac{\mathrm{Im}Y'(\omega_p)}{\mathrm{Re}Y(\omega_p)}. \qquad (3)$$

When applied to the mode representing the qubit, Eq. (3) gives an estimate for the Purcell limit on the qubit lifetime $T_1 = Q_{\rm qb}/\omega_{\rm qb}$ due to photons leaking out of the cavity.

In order to derive the effective low-energy quantum Hamiltonian of the circuit, we next neglect dissipation ($R_p \to \infty$) and introduce the normal (flux) coordinates $\phi_p(t) = f_p e^{j\omega_p t} + (f_p)^* e^{-j\omega_p t}$ associated with each LC oscillator in the equivalent circuit. We can then immediately write the classical Hamiltonian function of the equivalent circuit as $\mathcal{H}_0 = 2\sum_{p=1}^{M} (f_p)^* (L_p)^{-1} f_p$, where the subscript 0 indicates that we consider the linear part of the circuit. Kirchhoff's voltage law implies that up to an arbitrary constant, $\phi(t) = \sum_{p=1}^{M} \phi_p(t)$, where $\phi(t) = \int_{-\infty}^{t} V(\tau) d\tau$ is the flux coordinate of the junction with voltage $V(t)$. Note that by the second Josephson relation, the order parameter phase difference is related to the latter via $\varphi(t) = \phi(t)/\phi_0$ (modulo $2\pi$).

Quantization is achieved in the canonical way [22, 23] by replacing the flux amplitudes of the equivalent oscillators by operators as

$$f_p^{(*)} \to \sqrt{\frac{\hbar}{2} \mathcal{Z}_p^{\text{eff}}}\, a_p^{(\dagger)}, \quad \mathcal{Z}_p^{\text{eff}} = \frac{2}{\omega_p \text{Im} Y'(\omega_p)}, \tag{4}$$

with the dimensionless bosonic annihilation (creation) operators $a_p$ ($a_p^\dagger$). Direct substitution yields the Hamiltonian $H_0 = \sum_p \hbar\omega_p a_p^\dagger a_p$ of $M$ uncoupled harmonic oscillators (omitting the zero-point energies) and the Schrödinger operator of flux across the junction is

$$\hat{\phi} = \sum_{p=1}^{M} \sqrt{\frac{\hbar}{2} \mathcal{Z}_p^{\text{eff}}} \left(a_p + a_p^\dagger\right). \tag{5}$$

We emphasize that the harmonic modes $a_p$ represent collective excitations of the linear circuit and their frequencies $\omega_p$ are the equivalent of dressed oscillator frequencies. The coupling in the linear circuit is treated exactly and in particular no rotating wave approximation is used.

The Hamiltonian of the circuit including the JJ is then $H = H_0 + H_{\text{nl}}$, where $H_{\text{nl}} = -(\hat{\phi})^4/(24{\phi_0}^2 L_J) + \mathcal{O}((\hat{\phi}/\phi_0)^6)$. Physical insight may be gained by treating the nonlinear terms as a perturbation on top of $H_0$ assuming the eigenstates $|n_1, n_2, \ldots, n_M\rangle$ of the latter with energies $E^{(0)}_{n_1,n_2,\ldots,n_M} = \sum_i n_i \hbar\omega_i$, to be non-degenerate. Considering only the leading order $\phi^4$ nonlinearity, one then obtains the reduced Hamiltonian

$$H_4 = H_0' + \frac{1}{2} \sum_{pp'} \chi_{pp'} \hat{n}_p \hat{n}_{p'}. \tag{6}$$

Here $\hat{n}_p = a_p^\dagger a_p$ and $H_0' = H_0 + \sum_p \Delta_p \hat{n}_p$ includes a correction to the Lamb-shift given by $\Delta_p = -\frac{e^2}{2L_J}\left(\mathcal{Z}_p^{\text{eff}} \sum_q \mathcal{Z}_q^{\text{eff}} - (\mathcal{Z}_p^{\text{eff}})^2/2\right)$. We have further introduced the generalized $\chi$-shift $\chi_{pp'}$ between modes $p$ and $p'$. Clearly, $\alpha_p \equiv \chi_{pp}$ is the anharmonicity of the first excited state (self-Kerr) of mode $p$ while $\chi_{pp'} = \chi_{p'p}$ with $p \neq p'$ is the state-dependent frequency shift per excitation (cross-Kerr) of mode $p$ due to the presence of a single excitation in mode $p'$. Explicitly we find

$$\chi_{pp} = -\frac{L_p}{L_J}\frac{C_J}{C_p} E_C, \quad \chi_{pp'} = -2\sqrt{\chi_{pp}\chi_{p'p'}}. \tag{7}$$

Note that all modes acquire some anharmonicity due to the presence of the nonlinear JJ. There is thus no strict separation of qubit and cavity anymore. Colloquially, a mode with strong (weak) anharmonicity will be called qubit-like (cavity-like). Interestingly, in this lowest order approximation, the anharmonicity of mode $p$ is seen to be proportional to the inductive participation ratios [18] $i_p \equiv L_p/L_J$ and inversely proportional to the capacitive participation ratio $c_p \equiv C_p/C_J$. In the absence of a galvanic short of the junction in the resonator circuit, as is the case e.g. for a transmon qubit capacitively coupled to a cavity, it follows from the sum rule $\lim_{\omega\to 0}[Z(\omega)/(j\omega)] = \sum_p L_p = L_J$ that $i_p \leq 1$. Similarly, in the absence of any capacitance in series with $C_J$, it follows that $c_p \geq 1$, because $\lim_{\omega\to 0}[j\omega Z(\omega)] = \sum_p C_p^{-1} = C_\Sigma^{-1}$, where $C_\Sigma = C_J + C_\parallel$ and $C_\parallel$ is the total capacitance in parallel with $C_J$. Hence we see that in this experimentally relevant case, the effective anharmonicity of the qubit-like mode is always reduced as compared with the anharmonicity of the bare qubit given by $-E_C$ [11]. Remarkably, in this approximation we find (see Eq. (7)) that the cross-Kerr shift between two modes is twice the geometric mean of the anharmonicities of the two modes.

We emphasize that the above expressions do not however account for higher order effects in anharmonicity such as the change of sign of the cross-Kerr shift observed in the straddling regime [11, 24]. Such effects are however fully captured by the full model $H = H_0 + H_{\text{nl}}$, which can be solved numerically. Remarkably, because the *dressed* modes already resum all the *bare* harmonic modes, typically only a few dressed modes $M^* \ll M$ need to be included for good convergence, thus considerably reducing the size of the effective Hilbert space, which scales as $\prod_{p=1}^{M^*}(N_p + 1)$ where $N_p$ is the maximal allowed number of excitations in mode $p$ (e.g. $N_p = 1$ in a two-level approximation).

*Charge dispersion.* By assumption charge dispersion effects are neglected in the above approach. One may however ask how the charge dispersion of an *isolated* JJ is affected when the latter is coupled to a cavity. As in the Caldeira-Leggett model [25], the coupling between the JJ and Harmonic oscillators suppresses the probability of flux tunneling and hence reduces charge dispersion of the qubit further. A simple estimate of the suppression factor is provided by the probability $P_0$ of leaving the circuit in the ground state after a flux tunneling event and is found to be given by the "Lamb-Mössbauer" factor $P_0 \approx e^{-\frac{1}{2}\sum_{p\neq \text{qb}} \left(\frac{\delta q^2}{2C_p}\right)/(\hbar\omega_p)}$, where the sum excludes the qubit mode and $\delta q = C_J\phi_0/\tau$ is the charge (momentum) kick generated by a $\phi_0$ flux slip through the JJ of duration

| $\nu_{01}$ (GHz) | | $\nu_c$ (GHz) | | $\nu_{02}$ (GHz) | | $\alpha_{\rm qb}$ (MHz) | | $\chi$ (MHz) | | $L_J$ (nH) | $C_J$ (ff) |
|---|---|---|---|---|---|---|---|---|---|---|---|
| 7.77 | (7.763) | 8.102 | (8.105) | 15.33 | (15.333) | -210 | (-193) | −90 | (−80.6) | 5.83 | 7.6 |
| 7.544 | (7.54) | 8.126 | (8.05) | 14.808 | (14.830) | -280 | (-249) | −30 | (−33.0) | 6.12 | 9.2 |
| 7.376 | (7.376) | 7.858 | (7.864) | 14.489 | (14.495) | -264 | (-257) | −37.5 | (−38.7) | 6.67 | 4.0 |
| 7.058 | (7.045) | 8.005 | (8.023) | 13.788 | (13.794) | -328 | (-295) | −13.2 | (−13.3) | 7.45 | 5.2 |
| 6.808 | (6.793) | 8.019 | (8.017) | 13.286 | (13.294) | -330 | (-293) | −8 | (−8.4) | 7.71 | 7.8 |
| 6.384 | (6.386) | 7.832 | (7.823) | 12.45 | (12.449) | -318 | (-324) | −5.4 | (−7.6) | 9.40 | 0.34 |

TABLE I. Low-energy spectrum ($\nu_{01}$, $\nu_c$, $\nu_{02}$), qubit anharmonicity ($\alpha_{\rm qb}$) and state-dependent cavity shift ($\chi$) of six 3D-transmons. Results are shown in the format: experiment (theory). The theory values are obtained from a least square fit in $C_J$ of the numerically computed lowest three energy levels of the $\phi^6$ model. The fitted values of $C_J$ are given in the last column. Their order of magnitude (a few femto-farads) agrees with estimates based on the sizes of the junctions. The Josephson inductances $L_J$ are obtained from room-temperature resistance measurements of the junctions.

$\tau$ and $C_p = (1/2){\rm Im}Y'(\omega_p)$. Thus our assumption of neglecting charge dispersion of the qubit is well justified.

Interestingly though, each eigenmode of the system inherits some charge dispersion. This effect, essentially a consequence of hybridization, is of particular importance for applications such as quantum information storage in high-Q cavities coupled to JJs and is the subject of work in progress.

*Generalization to N junctions.* The approach can be extended to circuits with multiple JJs connected in parallel to a common linear circuit. Details about the derivation are given in the supplementary material [26] and we here only state the results. For $N$ qubits, the resonance frequencies of the linear part of the circuit are determined by the zeros of the admittance $Y_k(\omega) \equiv Z_{kk}(\omega)^{-1}$ for any choice of reference port $k = 1, \ldots, N$, where $\mathbf{Z}$ is the $N \times N$ impedance matrix of the linear part of the circuit with a port being associated with each junction. The flux operators of the $N$ junctions, with reference port $k$, are given by ($l = 1, \ldots, N$)

$$\hat{\phi}_l^{(k)} = \sum_{p=1}^{M} \frac{Z_{lk}(\omega_p)}{Z_{kk}(\omega_p)} \sqrt{\frac{\hbar}{2} \mathcal{Z}_{kp}^{\rm eff}} \left(a_p + a_p^\dagger\right), \qquad (8)$$

where $\mathcal{Z}_{kp}^{\rm eff} = 2/[\omega_p {\rm Im}Y_k'(\omega_p)]$. Note that the resonance frequencies are independent of the choice of reference port, while the eigenmodes do depend on it. In lowest order of PT and in the $\phi^4$ approximation, we find

$$\alpha_p = -12\beta_{pppp}, \quad \chi_{qp} = -24\beta_{qqpp}, \quad q \neq p, \qquad (9)$$

as well as the correction to the Lamb-shift $\Delta_p = 6\beta_{pppp} - 12\sum_q \beta_{qqpp}$. Here $\beta_{qq'pp'} = \sum_{s=1}^{N} \frac{e^2}{24 L_J^{(s)}} \xi_{sq}\xi_{sq'}\xi_{sp}\xi_{sp'}$, and choosing the first port as the reference port ($k = 1$), $\xi_{sp} = \frac{Z_{s1}(\omega_p)}{Z_{11}(\omega_p)} \sqrt{\mathcal{Z}_{1p}^{\rm eff}}$. Notice that the Cauchy-Schwarz inequality implies that $|\chi_{qp}| \leq 2\sqrt{\alpha_q \alpha_p}$. Also, if $q$ and $q'$ refer to two different qubit-like modes, then $\chi_{qq'}$ is a measure for the *total* interaction strength (cavity mediated and direct dipole-dipole coupling) between these two qubits.

*Comparison with experiment.* As a demonstration of this method, we apply it to the case illustrated in Fig. 1 of a single JJ coupled to a 3D cavity [3]. The admittance at the junction port $Y$ is a parallel combination of the linearized qubit admittance and the admittance $Y_c$ of the cavity-antenna system, i.e. $Y(\omega) = j\omega C_J - j/(\omega L_J) + Y_c(\omega)$. The junction is assumed to be dissipationless corresponding to a Purcell-limited qubit and ohmic losses of the cavity are included in $Y_c$, which is complex. The Josephson inductance $L_J$ is deduced from the measured junction resistance at room-temperature $R_T$, extrapolating it down to the operating temperature [27] of 15 mk and using the Ambegaokar-Baratoff relation, $E_J = h\Delta/(8e^2 R_T)$. $C_J$ – the only free parameter – is obtained by fitting the lowest three energy levels of the numerical solution of the $\phi^6$ model to the measured spectrum [3]. Although $Y_c$ may in principle be obtained from current-voltage measurements, this is not practical in this system, where the antenna is hard to access non-invasively, being inside a closed high-Q cavity. Instead we use a finite element High Frequency Simulation Software (HFSS) and obtain $Y_c(\omega)$ by solving the Maxwell equations numerically. Details on this simulation step are provided in the supplementary material [26].

From the zeros of the imaginary part of the admittance and their slopes we build and diagonalize the $\phi^6$ Hamiltonian in a truncated Hilbert space, keeping in total three dressed modes (one qubit and two cavity modes) and allowing for maximally ten excitations per mode. The results of fitting the low-energy spectrum of six different samples are presented in Table I, where we also compare the predicted and measured qubit anharmonicities and $\chi$-shifts. We find agreement with the measured spectrum at the sub per cent level and to within ten per cent with the measured anharmonicities and $\chi$-shifts.

*Conclusion and outlook.* We have presented a simple method to determine the effective low-energy Hamiltonian of a wide class of superconducting circuits containing lumped or distributed elements. This method is suitable for weakly nonlinear circuits, for which the normal modes of the linearized classical circuit provide a good basis in the quantum case. For an $N$ qubit system it requires only the knowledge of an $N \times N$ (classical) impedance matrix. By working in a basis of

dressed states, the parameters that appear in the Hamiltonian incorporate much of the renormalization induced by the coupling between a multi-level artificial atom and a multi-mode resonator. Consequently, the number of free parameters is considerably reduced as compared with standard models based on the Jaynes-Cummings paradigm expressed in terms of the experimentally inaccessible bare parameters. We have demonstrated the usefulness of this method in designing superconducting quantum information processing units by computing the low-energy spectrum of a 3D-transmon. Finally, this model may represent a suitable starting point for future investigations of the emerging ultra-strong coupling regime of cQED.

During completion of this work we became aware of related work by Bourassa et al. [28].

*Acknowledgments.* We thank Claudia De Grandi, Eustace Edwards and Mazyar Mirrahimi for discussions and Mikhael Guy from the Yale HPC center for support with numerical simulations. SEN acknowledges financial support from the Swiss NSF. HP, GK, BV, SS, LF, MD, RS and SG acknowledge financial support from IARPA, ARO (Contract W911NF-09-1-0514) and the American NSF (Contract DMR-1004406). All statements of fact, opinion or conclusions, contained herein are those of the authors and should not be construed as representing the official views or policies of IARPA, or the U.S. Government.

[1] M. H. Devoret and J. M. Martinis, Quantum Information Processing **3**, 1 (2004).
[2] A. Wallraff, , D. I. Schuster, A. Blais, L. Frunzio, R.-S. Huang, J. Majer, S. Kumar, S. M. Girvin, and R. J. Schoelkopf, Nature **431**, 162 (2004).
[3] H. Paik, D. I. Schuster, L. S. Bishop, G. Kirchmair, G. Catelani, A. P. Sears, B. R. Johnson, M. J. Reagor, L. Frunzio, L. I. Glazman, S. M. Girvin, M. H. Devoret, and R. J. Schoelkopf, Phys. Rev. Lett. **107**, 240501 (2011).
[4] M. Devoret, S. Girvin, and R. Schoelkopf, Ann. Phys **16**, 767 (2007).
[5] A. A. Houck, J. A. Schreier, B. R. Johnson, J. M. Chow, J. Koch, J. M. Gambetta, D. I. Schuster, L. Frunzio, M. H. Devoret, S. M. Girvin, and R. J. Schoelkopf, Phys. Rev. Lett. **101**, 080502 (2008).
[6] J. Bourassa, J. M. Gambetta, A. A. Abdumalikov, O. Astafiev, Y. Nakamura, and A. Blais, Phys. Rev. A **80**, 032109 (2009).
[7] T. Niemczyk, F. Deppe, H. Huebl, E. P. Menzel, F. Hocke, M. J. Schwarz, J. J. Garcia-Ripoll, T. H. D. Zueco, E. Solano, A. Marx, and R. Gross, Nature Physics **6**, 772 (2010).
[8] S. Filipp, M. Göppl, J. M. Fink, M. Baur, R. Bianchetti, L. Steffen, and A. Wallraff, Phys. Rev. A **83**, 063827 (2011).
[9] P. Nataf and C. Ciuti, Nature Communications **1** (2010), doi:10.1038/ncomms1069; O. Viehmann, J. von Delft, and F. Marquardt, Phys. Rev. Lett. **107**, 113602 (2011).
[10] A. Cottet, *Implementation of a quantum bit in a superconducting circuit*, Ph.D. thesis, Université Paris VI (2002).
[11] J. Koch, T. M. Yu, J. Gambetta, A. A. Houck, D. I. Schuster, J. Majer, A. Blais, M. H. Devoret, S. M. Girvin, and R. J. Schoelkopf, Phys. Rev. A **76**, 042319 (2007).
[12] J. A. Schreier, A. A. Houck, J. Koch, D. I. Schuster, B. R. Johnson, J. M. Chow, J. M. Gambetta, J. Majer, L. Frunzio, M. H. Devoret, S. M. Girvin, and R. J. Schoelkopf, Phys. Rev. B **77**, 180502 (2008).
[13] A. Blais, R.-S. Huang, A. Wallraff, S. M. Girvin, and R. J. Schoelkopf, Phys. Rev. A **69**, 062320 (2004).
[14] E. Jaynes and F. Cummings, Proceedings of the IEEE **51**, 89 (1963); M. Tavis and F. W. Cummings, Phys. Rev. **170**, 379 (1968).
[15] L. DiCarlo, J. M. Chow, J. M. Gambetta, L. S. Bishop, B. R. Johnson, D. I. Schuster, J. Majer, A. Blais, L. Frunzio, S. M. Girvin, and R. J. Schoelkopf, Nature **460** (2009), doi:10.1038/nature08121.
[16] In current realizations of the 3D-transmon qubits, the length of the antenna is between 1 and 10% of the wavelength of the fundamental bare cavity mode.
[17] M. D. Reed, L. DiCarlo, S. E. Nigg, L. Sun, L. Frunzio, S. M. Girvin, and R. J. Schoelkopf, Nature **482**, 382 (2012).
[18] V. E. Manucharyan, E. Boaknin, M. Metcalfe, R. Vijay, I. Siddiqi, and M. Devoret, Phys. Rev. B **76**, 014524 (2007).
[19] R. M. Foster, Bell System Technical Journal **3**, 260 (1924).
[20] E. R. Beinger, R. H. Dicke, N. Marcuvitz, C. G. Montgomery, and E. M. Purcell, *Principles of Microwave Circuits*, edited by C. G. Montgomery, R. H. Dicke, and E. M. Purcell (MIT Radiation Laboratory, 1945).
[21] The case of infinitely many discrete modes necessitates an extension of Foster's theorem as discussed in [29], but the results presented here still apply.
[22] M. H. Devoret, "Quantum fluctuations in electrical circuits," (Elsevier Science B. V., 1995) Chap. 10, p. 351, les Houches, Session LXIII.
[23] A. A. Clerk, M. H. Devoret, S. M. Girvin, F. Marquardt, and R. J. Schoelkopf, Rev. Mod. Phys. **82**, 1155 (2010).
[24] M. Boissonneault, J. M. Gambetta, and A. Blais, Phys. Rev. Lett. **105**, 100504 (2010).
[25] A. O. Caldeira and A. J. Leggett, Phys. Rev. Lett. **46**, 211 (1981).
[26] See supplementary material.
[27] K. Gloos, R. S. Poikolainen, and J. P. Pekola, Applied Physics Letters **77**, 2915 (2000).
[28] J. Bourassa, F. Beaudoin, J. M. Gambetta, and A. Blais, (2012), arXiv:1204.2237.
[29] M. K. Zinn, Bell System Technical Journal **31**, 378 (1951).